2024 IEEE 63rd Conference on Decision and Control (CDC)
December 16-19, 2024. MiCo, Milan, Italy

# Competitive Optimal Pricing Strategies for Charging Station Operators in the Frequency Containment Reserves Market

Guillaume Gasnier, Carlos Canudas-de-Wit

***Abstract*— We present an innovative strategy leveraging electric vehicles and their charging station infrastructure to provide grid-balancing services in the ancillary market. Our study focuses on the competition between two charging station operators for customer attraction and participation in the frequency containment reserves market. Our model tracks electric vehicles state-of-charge dynamics considering variables such as driver behavior, state-of-charge levels, and charging/discharging costs. Charging station operators participate in the frequency containment reserves market in collaboration with aggregators. We introduce an optimization framework coupled to game theory tools to determine pricing strategies that maximize profits for charging station operators. Our simulations demonstrate the benefits of charging stations participating in the frequency containment reserves market, whether competing or collaborating.**

## I. Introduction

The landscape of transportation and energy sectors is in the midst of a deep significant transformation. The surge in electric vehicle (EV) adoption and the network expansion of charging infrastructure mark a decisive pivot towards more eco-friendly transportation [1]. Simultaneously, the global shift towards renewable energy sources poses hurdles due to the intermittency of renewable energy sources, prompting the need for inventive energy storage remedies to tackle supply-demand imbalances [2]. Electric vehicles hold promise in fortifying grid stability, particularly with innovations like Vehicle-to-Grid (V2G) technology and swift responsiveness capabilities [3].

Considerable attention from researchers has been drawn to this domain. Kempton et al. [4] demonstrate the importance of specific attributes like minimal energy consumption, swift responsiveness and compensation based on availability rather than utilization for profitability within the EV sector. The European Commission highlights the significance of the primary reserve market, also known as "Frequency Containment Reserves" (FCR), in ensuring grid stability [5]. Hence, the EVs appears like an eco-friendly solution to include in the FCR market [6].

Recent research has extensively looked into the role that EVs could play in frequency regulation. Some studies look into the aggregation of vehicles via charging stations (CSs) [7]–[9], while others focus on individual benefits for EV users [10]–[12]. Economic evaluations conducted by researchers often factor in battery degradation within vehicles [8], [10]–[12]. Numerous papers analyze CS aggregators within the European FCR market [7], [8], with some leveraging V2G technology [8], [10]–[12], while others manage energy consumption diversely [7], [9]. Whereas, authors in [7] integrate additional battery storage with electric vehicles and authors in [9] use a mobility model to forecast CS occupancy.

Guillaume Gasnier, and Carlos Canudas-de-Wit are with CNRS, at GIPSA-lab, Grenoble, France (e-mail: {guillaume.gasnier, carlos.canudas-de-wit} @gipsa-lab.fr)

Previous studies did not explore scenarios in which two charging station operators (CSOs) in the same urban area compete for both the FCR market and customer attraction. In this study, we introduce an approach that leverages clusters of electric vehicle CSs participating in the ancillary market and easing network balancing services. This innovative contribution involves two CSOs (extensible to more) competing both in the FCR market and in vehicle attraction. This approach built upon our previous work [13] with a graph model derived under principles of mass conservation and energy balance, considering factors such as CS occupancy, average State of Charge (SoC) in each station, and energy exchanges with the grid. The attraction of CSs for EVs is based on various information such as the average SoC of vehicles and the price of each CS. Our approach employs various tools developed in game theory to compare different strategies for CSOs. We have designed different optimization problems associated with each strategy to maximize the gains of each CSO. Our work has demonstrated that collaboration among different CSOs maximizes their economic gains. However, this leads to increased charging prices for users and diminishes the capacity of CSs to participate in the FCR market.

## II. Auxiliary market

The FCR plays a key role in regulating grid frequency, preserving the stability of the power network. Positioned within the primary reserve category, FCR is rapid response capabilities, acting in less than 15 seconds. Participation in the primary reserve market requires the ability to dynamically adjust power consumption both upwards and downwards in response to grid frequency fluctuations. The FCR market operates at a European level, featuring diverse prices across individual countries determined by the matching of supply and demand. Market resolution occurs on a day-ahead basis, segmented into six time blocks of four hours each.

Fig. 1 illustrates two crucial time phases. During the Day-Ahead phase, market prices for the following day are determined. In this scenario, the CSO comprises two

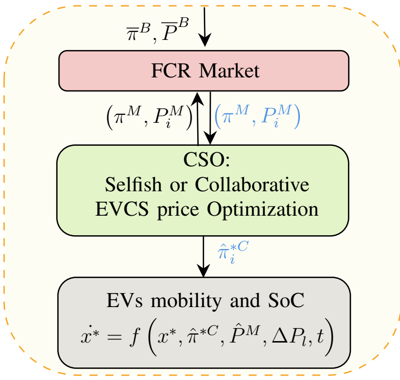


Fig. 1: Day-ahead, CSO declares capacity amount with price. EPEX spot market determines daily spot price evolution. FCR market reports retained capacity and price. CSO decides charging and discharging prices for EVs. Decision variables are in blue.

| | |
|---|---|
| **Demand** | |
| $\pi^D$ **(€/MW)** | [48,47,47,46,41,41,39,37,33,28,28,26,25,16,13,9,4,4,1,0] |
| $P^D$ **(MW)** | [31,22,36,17,1,16,38,17,22,12,22,28,16,8,13,31,23,4,27,34] |
| **Supply** | |
| $\pi^S$ **(€/MW)** | [2,5,5,8,8,9,12,13,13,15,16,17,18,20,22,29,32,42,45,46,46] |
| $P^S$ **(MW)** | [33,1,10,40,23,18,2,18,1,22,3,38,30,32,21,36,3,16,18,39] |

TABLE I: Demand and Supply Data.

charging stations. To participate in the FCR market, each CSO needs to submit the available power quantity $P_i^B \in \mathbb{N}$ in MW and the minimum compensation price $\pi_i^B \in \mathbb{R}$ in euros per megawatt (€/MW) for each time block. Here, $i \in \{1, 2\}$ represents the CS number. After the FCR market settlement, it provides the approved power quantity $P_i^M \in \mathbb{N}$ in MW and the price $\pi^M$ in €/MW. It is important to note that the returned price is the same for both CSOs. Moving to the Intraday phase, CSOs set the charging prices $\hat{\pi}_i^{*C}$ in €/kWh based on a differential equation $\hat{\dot{x}}^*$ using predictions of the return FCR market price, opponent CSO price, capacities sold in FCR market and grid regulations : $\hat{\pi}^M, \hat{\pi}^{*C}, \hat{P}^M$ and $\Delta\hat{P}_l$ for all time instance $t$. When a CSO participates in FCR, it must be able of both increasing and reducing its charging power. Additionally, the CSO must set the price $\hat{\pi}_i^{*C}$ in a manner that ensures there are always enough vehicles available to meet the grid operator's demands.

### A. FCR market settlement process

The FCR market settlement process involves solving two Linear Programming problems, as detailed in [13]. The first problem focuses on maximizing the amount of power exchanged, with the constraint that the highest bid price remains lower than the lowest asked price. The second problem determines the buying/selling price for all participants in the FCR market, aiming for an equitable outcome for everyone involved.

Table I serves as an illustrative example of organized offers in the FCR market for a 4-hour time window. The market resolution process is depicted in Fig. 2. Offers positioned before the intersection point of the demand curve and the supply curve are considered retained offers. Graphically, the price $\pi^M$ is determined at the intersection of the supply and demand curves. It is important to note that the values in this example are fictional, used for enhanced clarity and comprehension of Fig. 2. Additionally, Fig. 2 illustrates the evolution of the settled price in the FCR market for a day across the 6 time slots. There are other rules unused in this work to solve situation when two buyer/seller at the same price when there is not enough capacity to satisfy both.

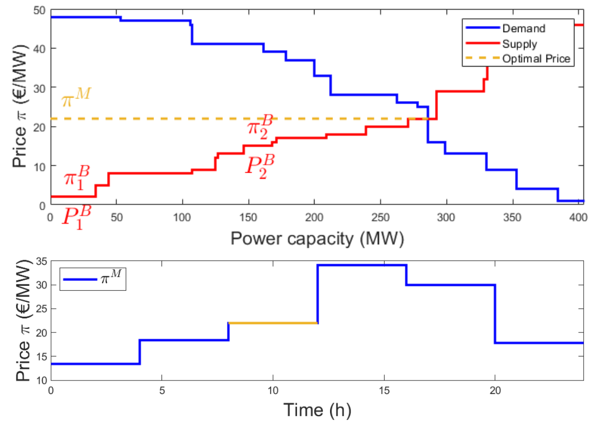


Fig. 2: FCR market price settlement based on Table I and Evolution of FCR prices during a day. In yellow, the price settled on top.

## III. EVs MOBILITY AND STATE-OF-CHARGE MODELS

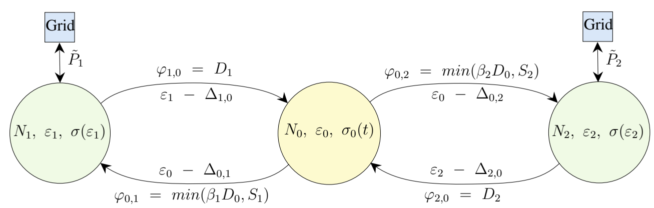


Fig. 3: Studied system mobility and energy visualisation. Yellow circles represent nodes, while green circles represent the aggregated charging stations.

The analyzed system, as depicted in Fig. 3, comprises a node connecting to two CSs equipped with both on-ramp and off-ramp capabilities. The influx of EVs seeking access to the CSs is divided based on factors such as the EVs' SoC and the current charging/discharging prices at each station. In our model, vehicles present at the CS are interlinked, allowing them to both charge and discharge. Following the completion of their charging, the outflow from the charging station returns to the node.

### A. Mobility model

The aggregated mobility model we used is formulated on a set of interconnected conservation Ordinary Differential Equations (ODEs) applicable to all time instances, denoted as $t$. Time is inherently implicit in all subsequent equations.

The representation of the number of EVs at node 0 and CSs at any specific time, expressed as $N_0$, $N_1$, and $N_2$, is

| Symbol | Description | Domain | Unit |
|---|---|---|---|
| $N$ | Number of EVs at node or CSs | $\mathbb{R}^+$ | veh |
| $\varphi_{i,j}$ | Flow from node or CS $i$ to $j$ | $\mathbb{R}^+$ | veh/h |
| $D$ | Demand function | $\mathbb{R}^+$ | veh/h |
| $S$ | Supply function | $\mathbb{R}^+$ | veh/h |
| $\sigma$ | Gating function | $[0,1]$ | - |
| $v$ | Vehicles exiting speed | $\mathbb{R}^+$ | veh/h |
| $\bar{\varphi}$ | Entering or exiting maximum flow | $\mathbb{R}^+$ | veh/h |
| $\omega$ | Vehicles entering speed | $\mathbb{R}^+$ | veh/h |
| $\bar{N}$ | Maximum capacity | $\mathbb{R}^+$ | veh |
| $\varepsilon$ | SoC | $[0,1]$ | - |
| $\varepsilon_l$ | SoC EVs start leaving CS | $[0,1]$ | - |
| $\beta$ | Split ratio | $[0,1]$ | - |
| $\pi^C$ | Charging/discharging price | $\mathbb{R}^+$ | €/kWh |
| $\pi^B$ | Capacity bid price | $\mathbb{R}^+$ | €/MW |
| $\pi^M$ | Capacity FCR market price | $\mathbb{R}^+$ | €/MW |
| $\tilde{P}$ | CS charging power | $\mathbb{R}$ | kW |
| $P_{CS}$ | Maximum CS charging power | $\mathbb{R}^+$ | kW |
| $\Delta$ | Travel energy loss | $[0,1]$ | - |
| $\Delta P$ | Power regulation | $\mathbb{R}$ | MW |
| $P^B$ | Capacity bid power | $\mathbb{R}^+$ | MW |
| $P^M$ | Capacity settled power | $\mathbb{R}^+$ | MW |
| $c$ | Average vehicle battery capacity | $\mathbb{R}^+$ | KWh |
| $c_i$ | Constants | $\mathbb{R}$ | - |

TABLE II: Notation summary of the model.

governed by the system

$$\Sigma_N : \begin{cases} \dot{N}_0 &= \varphi_{1,0} - \varphi_{0,1} + \varphi_{2,0} - \varphi_{0,2} & (1) \\ \dot{N}_1 &= \varphi_{0,1} - \varphi_{1,0} & (2) \\ \dot{N}_2 &= \varphi_{0,2} - \varphi_{2,0} & (3) \end{cases}$$

Where, $\varphi_{i,j}$ denotes the flow of EVs from node $i$ to node $j$. The flows entering $\mathrm{CS}_1$ and $\mathrm{CS}_2$ are represented by $\varphi_{0,1}$ and $\varphi_{0,2}$ while flows exiting CSs are respectively $\varphi_{1,0}$ and $\varphi_{2,0}$. The definitions for entering and exiting flows at the CSs are outlined below.

$$\varphi_{1,0} = \min\{D_1, S_0\} = D_1 \tag{4}$$

$$\varphi_{0,1} = \min\{\beta_1 D_0, S_1\} \tag{5}$$

$$\varphi_{2,0} = \min\{D_2, S_0\} = D_2 \tag{6}$$

$$\varphi_{0,2} = \min\{\beta_2 D_0, S_2\} \tag{7}$$

Where parameters $\beta_1$ and $\beta_2$ are split ratios. The demand functions $D_0$, $D_1$ and $D_2$ characterize the flow of EVs intending to depart, while the supply functions $S_0$, $S_1$ and $S_2$ represent the inflow that can be accommodated. For simplicity, congestion propagation in the origin/destination nodes is not considered, with the assumption that all demand can be entirely fulfilled at node 0. Consequently, except for equations (5) and (7), the expressions of (4) and (6) simplify as described above, with

$$D_0 = \sigma_0(t)\min\{v_0 N_0, \bar{\varphi}_0\} \tag{8}$$

$$D_1 = \sigma(\varepsilon_1)\min\{v_1 N_1, \bar{\varphi}_1\} \tag{9}$$

$$D_2 = \sigma(\varepsilon_2)\min\{v_2 N_2, \bar{\varphi}_2\} \tag{10}$$

$$S_1 = \min\{\omega(\bar{N}_1 - N_1), \bar{\varphi}_1\} \tag{11}$$

$$S_2 = \min\{\omega(\bar{N}_2 - N_2), \bar{\varphi}_2\} \tag{12}$$

Here, $\bar{N}_1$ and $\bar{N}_2$ represent the maximum capacity of each CS. $\bar{\varphi}_0$, $\bar{\varphi}_1$ and $\bar{\varphi}_2$ denote the maximum inflow/outflow for entering or leaving the node 0 and CSs. $\omega$ signifies the "speed" at which the CS fills. $\sigma(\varepsilon) \in [0,1]$ is a gating function depending of the average charge level $\varepsilon$ of all vehicles parking at the CS. We propose the following function:

$$\sigma(\varepsilon) = \begin{cases} 0, & \varepsilon < \varepsilon_l \\ \frac{\varepsilon - \varepsilon_l}{1 - \varepsilon_l}, & \varepsilon \geq \varepsilon_l \end{cases} \tag{13}$$

which allows the vehicles to leave (linearly) only after the Soc reaches the average value of $\varepsilon_l < 1$. The constants $v_1$ and $v_2$ define the speeds at which vehicles leave their respective nodes. For node 0, $v_0$ specifies the speed at which vehicles depart from the node. Additionally, $\sigma_0(t) \in [0,1]$ is time-dependent gating functions, as defined in [14]. It provides operational time profile during a day for the considered case.

The last parameters are the split ratios $\beta_1$ and $\beta_2$ based on the charging prices at the two CSs. Vehicles seeking to charge will be divided between $\mathrm{CS}_1$ and $\mathrm{CS}_2$. $\beta_1$ and $\beta_2$ and $g(x)$ are then defined as follows:

$$\beta_1(\pi_1^C, \pi_2^C) = g(\frac{\pi_1^C}{\pi_2^C})\beta \tag{14}$$

$$\beta_2 = \beta - \beta_1 \tag{15}$$

$$g(x) = (1 + e^{\frac{c4x-1}{c5}})^{-1} \tag{16}$$

Where $\beta$, determines the proportion of EVs that wish to charge, as defined in [9], [13] We assume that $\beta$ will depend on both the state of charge $\varepsilon_0$ and the lowest charging station price between $\pi_1^C$ and $\pi_2^C$

$$\beta(\pi_1, \pi_2, \varepsilon_0) = 1 - (1 + e^{-\gamma})^{-1} \tag{17}$$

with

$$\gamma = \gamma(\pi_1, \pi_2, \varepsilon_0) = \frac{\varepsilon_0 - c_1 + c_2 \min(\pi_1, \pi_2)}{c_3}$$

Fig. 4 illustrates the evolution of $\beta_1$ as a function of $\pi_1$ and $\pi_2$.

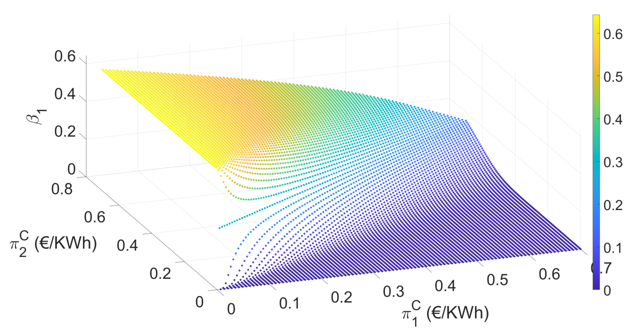


Fig. 4: Example of $\beta_1$ as a function of different charging station prices $\pi_1^C$ and $\pi_2^C$ . $c4 = 0.66$ and $c5 = 0.14$.

## B. Energy model

The power consumed by a charging station depends on the number of vehicles charging and the charging power. $\tilde{P}_i$ denotes the injected power in Kw from the grid at the CS $i$. It is defined as follows:

$$\tilde{P}_i = \begin{cases} 0, & \varepsilon = 1 \\ P_{CS_i} N_i + (\Delta P_i - P_i^M) & \varepsilon < 1 \end{cases} \tag{18}$$

The initial terms, $P_{CS_i} N_i$, represent the "nominal" power injected per charge station point, where $P_{CS_i}$ is the average power per charge point at CS $i$. The terms within the brackets express the disparity between the approved power $P_i^M$ as determined in the day-ahead and intraday markets, and $\Delta P_i$, which signifies the power requested by the TSO to the CSO at CS $i$ due to the mismatch between power supply and load demand. By definition, $\Delta P_i$ falls within the range of $[-P_i^M, P_i^M]$ and changes every 15 minutes. For the purpose of this study, we assume that $\Delta P_i$ is a random variable with $|\Delta P_i| \leq P_i^M$.

The average SoC at node 0 and CSs at any given time, denoted as $\varepsilon_0$, $\varepsilon_1$ and $\varepsilon_2$, respectivelly, are defined by system $\Sigma_\varepsilon$ defined below, and are obtained following the same procedure as in [13], *i.e.*

$$\Sigma_\varepsilon : \begin{cases} \dot{\varepsilon}_0 &= \frac{1}{N_0}\left[\varphi_{1,0}(-\varepsilon_0 + \varepsilon_1 - \Delta_{1,0}) + \right. \quad (19) \\ & \left. \varphi_{2,0}(-\varepsilon_0 + \varepsilon_2 - \Delta_{2,0})\right] \\ \dot{\varepsilon}_1 &= \frac{1}{N_1}\left[\varphi_{0,1}(-\varepsilon_1 + \varepsilon_0 - \Delta_{0,1}) + \frac{\tilde{P}_1}{c}\right] \quad (20) \\ \dot{\varepsilon}_2 &= \frac{1}{N_2}\left[\varphi_{0,2}(-\varepsilon_2 + \varepsilon_0 - \Delta_{0,2}) + \frac{\tilde{P}_2}{c}\right] \quad (21) \end{cases}$$

where $\Delta_{i,j}$ represents the traveling losses between the main node and the CSs (see Fig. 3).

## IV. Integrated Model

In this section we assemble the full model and show details on how all the parts in Fig. 1 will be connected.

### A. Mobility and SoC model

We rewrite the mobility and SoC model in a compact form, by defining $x \in \mathbb{R}^6$ as

$$x = [N_0, N_1, N_2, \varepsilon_0, \varepsilon_1, \varepsilon_2]^T \quad (22)$$

and

$$\dot{x} = \begin{bmatrix} f_N(x, \pi_1^C, \pi_2^C, t) \\ f_\varepsilon(x, \pi_1^C, \pi_2^C, P_1^M, P_2^M, \Delta P_1, \Delta P_2, t) \end{bmatrix} \quad (23)$$

$$\dot{x} = f(x, \pi_1^C, \pi_2^C, P_1^M, P_2^M, \Delta P_1, \Delta P_2, t) \quad (24)$$

where $f_N$, and $f_\varepsilon$ are the right hand function of systems $\Sigma_N$, and $\Sigma_\varepsilon$, respectively. Note that: $\pi_1^C$ and $\pi_2^C$ are our control variables to be optimized by the CSOs and they will be defined in the following section in connection with the optimization problem. We assumed that $\pi_1^C$ and $\pi_2^C$ are constants for a day.

### B. FCR market model

CSOs propose the bids pair $(P_{1,k}^B, \pi_{1,k}^B)$, $(P_{2,k}^B, \pi_{2,k}^B)$ for each 4 hours time instants $t_k = 4(k-1)[hr]$, where $k \in \mathbb{Z}_k \triangleq \{1, 2, \ldots, 6\}$. Then the FCR market settlement gives back the corresponding approved pair of power and prices $(P_{1,k}^M, \pi_k^M)$ and $(P_{2,k}^M, \pi_k^M)$.

CSOs aim to maximize their bids, $P_{1,k}^B$ and $P_{2,k}^B$, in order to increase their potential benefits with the predicted power of the connected Evs to the charging stations: $P_{CS_1}N_1(\tau)$ and $P_{CS_2}N_2(\tau)$, *i.e.*

$$P_{1,k}^B = \Phi(N_1(\tau)) \triangleq \min_{t_k < \tau < t_{k+1}} \left\{ \frac{P_{CS_1}N_1(\tau)}{2} \right\} \quad (25)$$

$$P_{2,k}^B = \Phi(N_2(\tau)) \triangleq \min_{t_k < \tau < t_{k+1}} \left\{ \frac{P_{CS_2}N_2(\tau)}{2} \right\} \quad (26)$$

where $\Phi$ is a function dependent on $N_1$ or $N_2$ that maximizes the allocated capacity (EVs flexibility) to enter into the FCR market. We take half of this capacity to be able to enter into the whole upward/downward regulation mechanism *i.e.* CSOs are then able to offer $\pm P_{1,k}^B, P_{2,k}^B$ power regulation. The bid prices $\pi_{1,k}^B$ and $\pi_{2,k}^B$, are in general set from complex economic mechanics which go beyond this study. In this work we assume that $\pi_{1,k}^B = \pi_{2,k}^B = 0$, so that all the bid offers $P_{1,k}^B$ and $P_{2,k}^B$ will be retained during the market settlement process. Therefore, we have

$$P_{1,k}^M = P_{1,k}^B, \quad P_{2,k}^M = P_{2,k}^B \quad \forall k \in \mathbb{Z} \quad (27)$$

Finally the returned price from the FCR market is given by:

$$\pi_k^M = \Psi(P_{1,k}^B, \pi_{1,k}^B, P_{2,k}^B, \pi_{2,k}^B) \quad (28)$$

where $\Psi$ represents the map associated to the optimisation problem settling the FCR market.

### C. TSO power requests

The last components to be defined in the model (which introduces a time-dependence in the right hand side of equation (24)) are $\Delta P_1(t) \in [-P_1^M, P_1^M]$ and $\Delta P_2(t) \in [-P_2^M, P_2^M]$ . They describe the real-time power requested by the TSO to the CSO to both CSs. These power requests are related to the mismatch between power supply and load demand, and it is mainly due to the renewable energy sources (RES) uncertain production, among other factors. Here we modeled $\Delta P_1(t)$ and $\Delta P_2(t)$ as discrete functions with time steeps $t_l$:

$$\Delta P_{1,l} \triangleq \text{Rand}_l \cdot P_{1,k}^M \quad (29)$$

$$\Delta P_{2,l} \triangleq \text{Rand}_l \cdot P_{2,k}^M \quad (30)$$

where $\text{Rand}_l$ represents a random number between $[-1, 1]$ with an uniform distribution. Each realization of $\text{Rand}_l$ is done every 15 min at time instants $t_l = (l-1)/4[hr]$, where $l \in \mathbb{Z}_l \triangleq \{1, 2, \ldots, 96\}$, as imposed by the TSO during the real-time operation, see [5]. $\text{Rand}_l$ is required to exhibit diversity in its values to prevent an excessive concentration of negative or positive values.

### D. Integrated model

Integration to previous components in the general model (24) gives, $\forall \tau \in \mathbb{I}_k \triangleq [t_k, t_{k+1})$, $k \in \mathbb{Z}_k$, $l \in \mathbb{Z}_l$

$$\boxed{\dot{x}(t) = f(x(t), \pi_1^C, \pi_2^C, \Phi(x(\tau)), \Delta P_{1,l}, \Delta P_{2,l}, t)} \quad (31)$$

where $\Phi(x(\tau)) = [\Phi(N_1(\tau)), \Phi(N_2(\tau))] = [P_{1,k}^M, P_{2,k}^M]$.

*Remark 1:* Unlike conventional actors in the FRC market, which have backup power from generators under their control, the power supply for a CSO depends on the mobility of EVs and their presence at the charging station. Therefore, it is crucial for the CSO to have an electromobility model that can forecast the potential occupancy at the CS. This prediction, in turn, allows for the calculation of the variables $P_1^M$ and $P_2^M$ for participation in the day-ahead market

*Remark 2:* Note that solving equation (31) is not a straightforward task, primarily due to non-causal components stemming from the computation of $P_{1,k}^M$ and $P_{2,k}^M$.

Additionally, it contains random elements that arise from $\Delta P_{1,l}$ and $\Delta P_{2,l}$.

Under the fact that $\Delta P_{1,l} \leq P_1^M$ and $\Delta P_{2,l} \leq P_2^M$, are unknown, but upper bounds are known by construction, and given by $|\Delta P_{1,l}| \leq P_1^M$ and $|\Delta P_{2,l}| \leq P_2^M$, these bounds result in additional inequality constraints in an optimization problem.

*Problem 1:* Solving the differential equation (31) can be approximate by solving an optimization problem. The Best possible feasible solution (in the sense of considering both the upper and lower bounds of the random variables $\Delta P_{1,l}$ and $\Delta P_{2,l}$, and accounting for the non-causal components $P_{1,k}^M$ and $P_{2,k}^M$ ) for solving the differential equation (31) is given by the solution of the following optimization problem.

$\mathbb{P}_1$: $\forall\ k \in \mathbb{Z}_k,\ l \in \mathbb{Z}_l$ solve:

$$\hat{P}_1^M, \hat{P}_2^M = \max_{\lambda_1,\lambda_2} \sum_{k=1}^{6} (\lambda_{1,k} + \lambda_{2,k}) \tag{32}$$

under

$$\dot{\hat{x}}(t) = f(\hat{x}(t), \pi_1^C, \pi_2^C, \lambda_{1,k}, \lambda_{2,k}, \Delta\hat{P}_{1,l}, \Delta\hat{P}_{2,l}, t) \tag{33}$$

$$0 \leq \lambda_{1,k} \leq \min_{\tau \in \mathbb{I}_k} \left\{ \frac{P_{CS_1}\hat{N}_1(\tau)}{2} \right\} \tag{34}$$

$$0 \leq \lambda_{2,k} \leq \min_{\tau \in \mathbb{I}_k} \left\{ \frac{P_{CS_2}\hat{N}_2(\tau)}{2} \right\} \tag{35}$$

$$\Delta\hat{P}_{1,l} \leq \lambda_{1,k}, \quad \Delta\hat{P}_{1,l} \geq -\lambda_{1,k} \tag{36}$$

$$\Delta\hat{P}_{2,l} \leq \lambda_{2,k}, \quad \Delta\hat{P}_{2,l} \geq -\lambda_{2,k} \tag{37}$$

where $\Delta\hat{P}_{1,l}$ and $\Delta\hat{P}_{2,l}$ act here as slack variables.

## V. Optimal energy-price strategy

Within this section, we begin by presenting the utility function earmarked for optimization. Following that, we formulate the two considered problems. One for non-cooperative CSOs and the second for cooperative CSOs. We also put forward a feasible forecasting model, along with an upper limit on utility to guide the optimization procedure. Lastly, we outline and propose a solution for the optimal energy-price optimization problem.

### A. Utility function

For each day, $CSO_1$ and $CSO_2$ must set a price $\pi_1^C$ and $\pi_2^C$ while seeking to maximize their gains achieved during the day. CSOs have two different sources of revenue. The first source is the earnings from selling energy to EVs, given by $\int_0^T \pi_1^C \tilde{P}_1$ and $\int_0^T \pi_2^C \tilde{P}_2$, while the second source is the earnings from selling capacity in the FCR market, which is calculated as $\sum_{k=1}^6 \pi_k^M P_{1,k}^M$ and $\sum_{k=1}^6 \pi_k^M P_{2,k}^M$ for each 4-hour block $k$. The cost functions $J_1$ and $J_2$ are defined :

$$J_1 = \int_0^T \pi_1^C \tilde{P}_1 dt + \sum_{k=1}^{6} \pi_k^M P_{1,k}^M \tag{38}$$

$$J_2 = \int_0^T \pi_2^C \tilde{P}_2 dt + \sum_{k=1}^{6} \pi_k^M P_{2,k}^M \tag{39}$$

However, $\tilde{P}_1$ and $\tilde{P}_2$ depend on $\Delta P_1$ and $\Delta P_2$, which are missing pieces of information during optimization. From the definition of $\tilde{P}_1$ and $\tilde{P}_2$, and the fact that $-P_1^M \leq \Delta P_1 \leq P_1^M$ and $-P_2^M \leq \Delta P_2 \leq P_2^M$, we have

$$\tilde{P}_1 = P_{CS_1}N_1 + (\Delta P_1 - P_1^M) \leq P_{CS_1}N_1 \tag{40}$$

$$\tilde{P}_2 = P_{CS_2}N_2 + (\Delta P_2 - P_2^M) \leq P_{CS_2}N_2 \tag{41}$$

Therefore, we have the functions $\hat{J}_1$ and $\hat{J}_2$ that calculates an upper bound of $J_1 \leq \hat{J}_1$ and $J_2 \leq \hat{J}_2$ for the full day, *i.e.* $t \in [0, T]$, with $T = 24$ hrs:

$$\hat{J}_1(\hat{x}, \pi_1^C, \hat{P}_1^M, \pi_{\max}^M) = \int_0^T \pi_1^C P_{CS_1}\hat{N}_1 dt + \pi_{\max}^M \sum_{k=1}^{6} \hat{P}_{1,k}^M \tag{42}$$

$$\hat{J}_2(\hat{x}, \pi_2^C, \hat{P}_2^M, \pi_{\max}^M) = \int_0^T \pi_2^C P_{CS_2}\hat{N}_2 dt + \pi_{\max}^M \sum_{k=1}^{6} \hat{P}_{2,k}^M \tag{43}$$

where $\pi_{max}^M$ is an upper bound on $\pi_k^M$, while $\hat{N}_1$, $\hat{N}_2$, $\hat{P}_{1,k}^M$ and $\hat{P}_{2,k}^M$ are obtained from Problem $\mathbb{P}_1(\pi_1^C, \pi_2^C)$.

*Remark 3:* Note that evaluation of the real benefits need to be done using the true cost functions $J_1$ and $J_2$, which is done by replacing the computed optimal price $\hat{\pi}_1^{*C}, \hat{\pi}_2^{*C}$ and $\hat{P}_1^M, \hat{P}_2^M$ obtained from CSO1 and CSO2's pricing strategies (in section V-B),in the ground true equation (31), *i.e.*

$$\dot{x}^*(t) = f(x^*(t), \hat{\pi}_1^{*C}, \hat{\pi}_2^{*C}, \hat{P}_1^M, \hat{P}_2^M, \Delta P_{1,l}, \Delta P_{2,l}, t) \tag{44}$$

And finally using this ground true solution to evaluate the effective utility benefits $J_1^*(x^*, \hat{\pi}_1^{*C}, \hat{P}_1^M, \pi^M)$ and $J_2^*(x^*, \hat{\pi}_2^{*C}, \hat{P}_2^M, \pi^M)$. Note that this value will depend on the particular sequences $\Delta P_{1,l}$ and $\Delta P_{2,l}$ resulting from the day profile difference between power demand and power production variability.

$$J_1^*(x^*, \hat{\pi}_1^{*C}, \hat{P}_1^M, \pi^M) = \int_0^T \hat{\pi}_1^{*C} \tilde{P}_1 dt + \sum_{k=1}^{6} \pi_k^M \hat{P}_{1,k}^M \tag{45}$$

$$J_2^*(x^*, \hat{\pi}_2^{*C}, \hat{P}_2^M, \pi^M) = \int_0^T \hat{\pi}_2^{*C} \tilde{P}_1 dt + \sum_{k=1}^{6} \pi_k^M \hat{P}_{2,k}^M \tag{46}$$

We will explore two scenarios: one, non-collaborative, where CSOs setting their prices independently, and another where they collaborate, exchanging informations to find the optimal prices. The first scenario emphasizes individual strategies for profit maximization, while the second prioritizes collective prosperity alongside individual gains.

### B. Competitive Pricing Strategies

In the scenario where CSOs are in competition and both must set a price simultaneously while ignoring the price of the other CSO, they will develop a MaxiMin strategy for non zero-sum game [15].

*Problem 2:* MaxiMin strategy means for $CSO_1$ choose a price $\pi_1^C$ to maximize its profit, over $CSO_2$'s worst-case

| Symbol | Value | Unit | Symbol | Value | Unit |
|---|---|---|---|---|---|
| $w$ | 50 | km/h | $\varepsilon_l$ | 0.8 | - |
| $v_0, v_1, v_2$ | 50 | km/h | $P_{CS_1}, P_{CS_2}$ | 40 | kW |
| $\varphi_0, \varphi_1, \varphi_2$ | 10000 | veh/h | $c$ | 40 | kWh |
| $\bar{N}_0, \bar{N}_1, \bar{N}_2$ | 10000 | veh | $\Delta_{ij}$ | 0.4 | - |
| $c_1$ | 0.83 | - | $c_4$ | 1 | - |
| $c_2$ | 1.3 | - | $c_5$ | 0.14 | - |
| $c_3$ | 0.06 | - | | | |

TABLE III: Simulation parameters and their values.

response *i.e.* $\text{CSO}_1$ is aware of the full range of possible prices for $\text{CSO}_2$ ($\pi_2^C \in \Pi^C$). We have $\pi_1^{*C}$ the result of MaxiMin for $\text{CSO}_1$ defined as:
$\mathbb{P}_2$: $\forall\ k \in \mathbb{Z}_k,\ l \in \mathbb{Z}_l$ solve:

$$\hat{\pi}_1^{*C} = \max_{\pi_1^C \in \Pi^C} \min_{\pi_2^C \in \Pi^C} \hat{J}_1 \quad \text{under} \quad \mathbb{P}_1(\pi_1^C, \pi_2^C) \tag{47}$$

and by symmetry

$$\hat{\pi}_2^{*C} = \max_{\pi_2^C \in \Pi^C} \min_{\pi_1^C \in \Pi^C} \hat{J}_2 \quad \text{under} \quad \mathbb{P}_1(\pi_1^C, \pi_2^C) \tag{48}$$

### C. Cooperative Pricing Strategies

In this scenario, the CSOs collaborate, meaning there is an exchange of information when they choose their prices. Pooling profits from CSOs can result in significant disparity in profit distribution, as each CSO seeks to maximize its own gains, even in collaboration. Therefore, instead of summing up, the profits are multiplied together to reflect this individual profit maximization.

*Problem 3:* The computable optimal energy-price strategy for cooperative CSOs consists in solving the following optimal problem.
$\mathbb{P}_3$: $\forall\ k \in \mathbb{Z}_k,\ l \in \mathbb{Z}_l$ solve:

$$\hat{\pi}_1^{*C}, \hat{\pi}_2^{*C} = \max_{\pi_1^C, \pi_2^C \in \Pi^C} \hat{J}_1 \hat{J}_2 \quad \text{under} \quad \mathbb{P}_1(\pi_1^C, \pi_2^C) \tag{49}$$

Where $\hat{\pi}_1^{*C}$ and $\hat{\pi}_2^{*C}$ are the optimal solutions for a collaborative strategy.

## VI. Simulation Results

This section compares the collaborative and competitive approaches from the perspectives of key stakeholders: the CSO, EV users, and the FCR market.

Let $\pi_1^C$ and $\pi_2^C \in \Pi^C \triangleq \{0.22, 0.24, 0, 26, \ldots, 0.34\}$, with $\Pi^C$ being the admissible set for $\pi_1^C$ and $\pi_2^C$. We use a greedy approach to solve problems $\mathbb{P}_2$ and $\mathbb{P}_3$, providing a comprehensive overview of potential solutions. Consider the following experiment with systems parameters in Table III. Initial values of the system are $N_0(0) = 6000$, $N_1(0) = 2000$, $N_2(0) = 2000$, $\varepsilon_0(0) = 0.6$, $\varepsilon_1(0) = 0.8$ and $\varepsilon_2(0) = 0.8$.

1) For all $\pi_1^C, \pi_2^C \in \Pi^C$ we solve problem $\mathbb{P}_1$ (*i.e.* $\hat{P}_1^M$ and $\hat{P}_2^M$) and we compute cost functions $\hat{J}_1$ and $\hat{J}_2$.
2) From these results we easily compute $\hat{J}_1^*$, $\hat{J}_2^*$ from problem $\mathbb{P}_2$ and $\hat{J}_1^* \hat{J}_2^*$ from problem $\mathbb{P}_3$.

We will use the following notations to distinguish the results of problem $\mathbb{P}_2$ and $\mathbb{P}_3$ and $\text{CS}_1$ and $\text{CS}_2$. $\pi_{1,\mathbb{P}_2}^{*C}$ and $\pi_{2,\mathbb{P}_2}^{*C}$ respectively correspond to the results of $\mathbb{P}_2$ for $\text{CS}_1$ and $\text{CS}_2$. As well as $\pi_{1,\mathbb{P}_3}^{*C}$ and $\pi_{2,\mathbb{P}_3}^{*C}$ for $\mathbb{P}_3$. We also have $\hat{J}_{1,\mathbb{P}_2}^*$, $\hat{J}_{2,\mathbb{P}_2}^*$, $\hat{J}_{1,\mathbb{P}_3}^*$ and $\hat{J}_{2,\mathbb{P}_3}^*$ for associated cost functions.

When charging stations are in competition, after solving problem $\mathbb{P}_2$ , we obtain $\pi_{1,\mathbb{P}_2}^{*C}$ = $\pi_{2,\mathbb{P}_2}^{*C}$ = 0.22 €/kWh (pink circle in figures 5a and 5b). We then have $\hat{J}_{1,\mathbb{P}_2}^* = \hat{J}_{2,\mathbb{P}_2}^* = 4.3 \times 10^5$.

When charging stations collaborate, we can observe from Fig. 5c that there are two global maxima (green circles in figures 5c). Then, $(\pi_{1,\mathbb{P}_3}^{*C}, \pi_{2,\mathbb{P}_3}^{*C}) \in \{(0.30, 0.34), (0.34, 0.30)\}$. In the remainder of this section, we will consider the result $\pi_{1,\mathbb{P}_3}^{*C}$ = 0.30 €/kWh and $\pi_{2,\mathbb{P}_3}^{*C}$ = 0.34 €/kWh as the outcome of problem $\mathbb{P}_3$. There is an increase of 36% between $\pi_{1,\mathbb{P}_2}^{*C}$ and $\pi_{1,\mathbb{P}_3}^{*C}$, as well as an increase of 54% between $\pi_{2,\mathbb{P}_2}^{*C}$ and $\pi_{2,\mathbb{P}_3}^{*C}$. Consequently, we have $\hat{J}_{1,\mathbb{P}_3}^* = 1.3 \times 10^6$ and $\hat{J}_{2,\mathbb{P}_3}^* = 0.6 \times 10^6$. This represents an increase of 202% from $J_{1,\mathbb{P}_2}^*$ to $J_{1,\mathbb{P}_3}^*$ and 40% for from $J_{2,\mathbb{P}_2}^*$ to $J_{2,\mathbb{P}_3}^*$.

In Fig. 6 top, we can observe benefits for CSOs during a day. $\mathcal{N}_{0.22}$ represents earnings for both CSs in problem $\mathbb{P}_2$ while $\mathcal{N}_{0.30}$ and $\mathcal{N}_{0.34}$ are benefits for $\text{CS}_1$ and $\text{CS}_2$ in problem $\mathbb{P}_3$. We observe that the solution to problem $\mathbb{P}_2$, where $\text{CS}_1$ and $\text{CS}_2$ have equal prices, implies that the total reserve capacity sold to the FCR market ($\sum_{k=1}^6 P_1^M = \sum_{k=1}^6 P_2^M = 501\text{MW}$) is greater than the solution to problem $\mathbb{P}_3$, where CSs have different prices ($\sum_{k=1}^6 P_1^M = 335\text{MW}$ and $\sum_{k=1}^6 P_2^M = 201\text{MW}$). This results in a difference of 41% for $\text{CS}_1$ and 149% for $\text{CS}_2$. This translates to the gains of $\text{CS}_1$ and $\text{CS}_2$ at $\pi_{1,\mathbb{P}_2}^{*C} = \pi_{2,\mathbb{P}_2}^{*C} = 0.22$ being higher than the gains of CSs at $\pi_{1,\mathbb{P}_3}^{*C} = 0.30$ and $\pi_{2,\mathbb{P}_3}^{*C} = 0.34$ at time $t = 0$ but is not significant compared to total earnings in a day. Furthermore, in Fig. 6 bottom, we can observe that the number of vehicles served by the $\text{CS}_1$ $\mathcal{N}$ is significantly higher in $\mathbb{P}_3$ solution ($\mathcal{N}_{0.30}(24) \approx 112000$) compared to $\mathbb{P}_2$ solution ($\mathcal{N}_{0.22}(24) \approx 60000$) and $\text{CS}_2$ in $\mathbb{P}_3$ has slightly fewer vehicles $\mathcal{N}_{0.34}(24) \approx 53000$. This is reflected in the gains of the CSs.

Based on these results, we can argue that with a collaborative strategy, CSs have an incentive to set a higher charging price and participate less in the FCR market compared to a competitive strategy. The price of FCR capacity is not high enough to offset the losses associated with longer charging duration. Indeed, when CSs are in competition, it allows for a lower price for users and an increase in the capacity reserve sold to the FCR market.

## VII. Conclusions

In this study, we have presented an approach to integrate various CSOs into the FCR market using a mobility model, aggregated charging stations, and an FCR market model. Despite the complexity of our problem with different time scales, we have proposed various pricing strategies in cases where charging stations are in competition or cooperation. Our results have shown that if charging stations are in

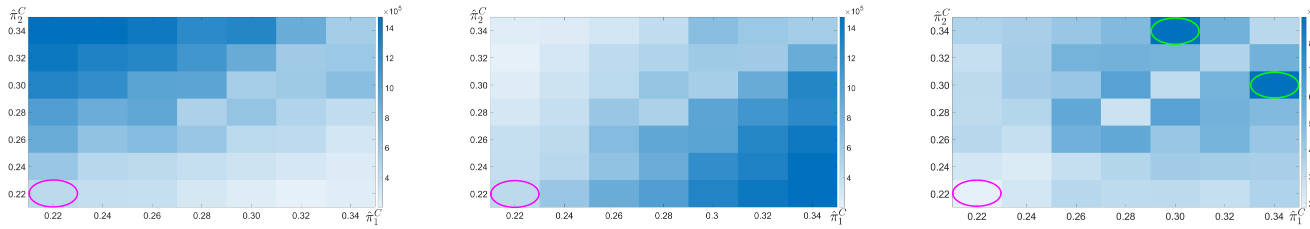

(a) Cost function upper bound $\hat{J}_1$ (€). (b) Cost function upper bound $\hat{J}_2$ (€). (c) Cost function upper bound $\hat{J}_1\hat{J}_2$.

Fig. 5: a) Numerical results from problem $\mathbb{P}_1$ for $CS_1$, b) Numerical results from problem $\mathbb{P}_1$ for $CS_2$ and c) Numerical result for cost function $\hat{J}_1\hat{J}_2$ ◯ Optimal solution from problem $\mathbb{P}_2$ and ◯ Optimal solution from problem $\mathbb{P}_3$.

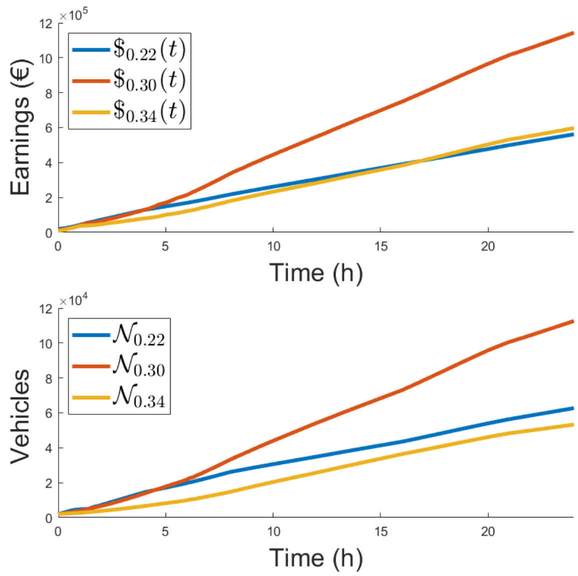


Fig. 6: Numerical results from problems $\mathbb{P}_2$ and $\mathbb{P}_3$. Top figure presents the comparison of gains over time for different stations for each problem. Bottom figure depicts the number of vehicles served over time in each station for each problem.

competition, it is beneficial for users who pay a lower price and for the FCR market, which receives more capacity to sell. Conversely, cooperation is advantageous for CSOs as it allows them to significantly increase their profits. A future avenue of research could involve extending this work to a larger-scale mobility model [16] and potentially more CSOs in competition.

## References


[1] A. Razmjoo, A. Ghazanfari, M. Jahangiri, *et al.*, "A comprehensive study on the expansion of electric vehicles in europe," *Applied Sciences*, vol. 12, no. 22, p. 11 656, 2022.

[2] A. Clerjon and F. Perdu, "Matching intermittent electricity supply and demand with electricity storage-an optimization based on a time scale analysis," *Energy*, vol. 241, p. 122 799, 2022.

[3] S. S. Ravi and M. Aziz, "Utilization of electric vehicles for vehicle-to-grid services: Progress and perspectives," *Energies*, vol. 15, no. 2, p. 589, 2022.

[4] W. Kempton and J. Tomić, "Vehicle-to-grid power fundamentals: Calculating capacity and net revenue," *Journal of power sources*, vol. 144, no. 1, pp. 268–279, 2005.

[5] Interrface. "Tso-dso-consumer interface architecture to provide innovative grid services for an efficient power system." (2019), [Online]. Available: https://ec.europa.eu/research/participants/documents/downloadPublic?documentIds=080166e5c735ee44&appId=PPGMS (visited on 11/02/2023).

[6] P. Codani, M. Petit, and Y. Perez, "Participation of an electric vehicle fleet to primary frequency control in france," *International Journal of Electric and Hybrid Vehicles*, vol. 7, no. 3, pp. 233–249, 2015.

[7] X. Duan, Z. Hu, and Y. Song, "Bidding strategies in energy and reserve markets for an aggregator of multiple ev fast charging stations with battery storage," *IEEE Transactions on Intelligent Transportation Systems*, vol. 22, no. 1, pp. 471–482, 2020.

[8] S.-A. Amamra and J. Marco, "Vehicle-to-grid aggregator to support power grid and reduce electric vehicle charging cost," *IEEE Access*, vol. 7, pp. 178 528–178 538, 2019.

[9] M. Čičić, G. Gasnier, and C. Canudas-de-Wit, "Electric Vehicle Charging Station Pricing Control under Balancing Reserve Capacity Commitments," in *CDC 2023 - 62nd IEEE Conference on Decision and Control*, Singapour: IEEE, Dec. 2023, pp. 1–7.

[10] K. Kaur, N. Kumar, and M. Singh, "Coordinated power control of electric vehicles for grid frequency support: Milp-based hierarchical control design," *IEEE transactions on smart grid*, vol. 10, no. 3, pp. 3364–3373, 2018.

[11] O. Kolawole and I. Al-Anbagi, "Electric vehicles battery wear cost optimization for frequency regulation support," *IEEE Access*, vol. 7, pp. 130 388–130 398, 2019.

[12] A. O. David and I. Al-Anbagi, "Evs for frequency regulation: Cost benefit analysis in a smart grid environment," *IET Electrical Systems in Transportation*, vol. 7, no. 4, pp. 310–317, 2017.

[13] G. Gasnier and C. Canudas-de-Wit, "Optimal pricing strategies for charging stations in the frequency containment reserves market for vehicle-to-grid integration," Accepted to *European Control Conference* June 2024, EUCA, 2024.

[14] M. Rodriguez-Vega, C. Canudas-de-Wit, G. De Nunzio, and B. Othman, "A graph-based mobility model for electric vehicles in urban traffic networks: Application to the grenoble metropolitan area," in *2023 European Control Conference (ECC), Bucarest, Rumania*, IEEE, 2023, pp. 1–8.

[15] J. Von Neumann and O. Morgenstern, *Theory of games and economic behavior (60th Anniversary Commemorative Edition)*. Princeton university press, 2007.

[16] C. Canudas de Wit and B. Lefeuvre, "Emob-twin: A digital twin for electromobility flexibility forecast ⋆," 2024.